UNIVERSITY OF CALIFORNIA,
IRVINE

Cancer stem cells, radiotherapy and the emergence of resistance: The effect of feedback and reprogramming

THESIS

submitted in partial satisfaction of the requirements
for the degree of

MASTER OF SCIENCE

in Mathematical and Computational System Biology

by

Na Yeon Kim

Thesis Committee:
Chancellor Professor John Lowengrub, Chair
Chancellor Professor Natalia Komarova
Professor Long Chen

2019

TABLE OF CONTENTS

LIST OF FIGURES

LIST OF EQUATIONS

LIST OF TABLES

ACKNOWLEDGMENTS

Foremost, I would like to express the deepest appreciation to my committee chair, Professor John Lowengrub for the support of my master study and research. He continually and convincingly supports me with his patience, motivation, enthusiasm and immense knowledge. His guidance and persistent helped in all the time of research and writing of this thesis. I could not have imagined having a better advisor and mentor for my Master's degree.

Besides my advisor, I would like to thank my committee members, Professor Long Chen and Professor Natalia Komarova, for their encouragement, insightful comments and intuitive questions.

I would also thank to the University of California at Los Angeles for permission to include copyrighted photographs as part of my thesis. I

Last but not least, I would like to thank to my family for supporting me mentally and spiritually throughout my life.

ABSTRACT OF THE THESIS

Cancer stem cells, radiotherapy and the emergence of resistance:
The effect of feedback and reprogramming

By

Na Yeon Kim

Master of Science in Mathematical and Computational System Biology

University of California, Irvine, 2019

Professor John Lowengrub, Chair

There is increasing evidence that cancer stem cells (CSC) are more radioresistant than differentiated cancer cells (DCC). Radiation treatment of solid tumors can induce long-term enrichment of CSC, which can lead to resistance and a loss of sensitivity to radiotherapy. At the same time, radiation-induced reprogramming of DCCs into CSCs has also been observed. Using a mathematical model, we study the dynamics of CSCs and DCCs with reprogramming induced by radiation therapy. We also investigate the effect of feedback on cell division rates together with reprogramming, and renewal probability. We observe that feedback on cell division rates results in long-term enrichment of CSC whereas the effect of feedback on self-renewal probabilities results only in short-term CSC enrichment even when there is reprogramming. In the context of glioblastoma, we find there is an optimal choice of dose fractionation to reduce CSC percentages and tumor sizes.

1. INTRODUCTION

One of the most prevalent sources of tumor heterogeneity is the small population of cancer stem cells (CSCs) within solid tumors (1). Unlike most of the cells in a tumor, CSCs have the ability to regenerate a tumor. Further, the presence of CSCs and tumor heterogeneity leads to variable growth patterns and responses to treatment as CSCs are typically more radioresistant than non-CSC. Increased frequency of CSCs in a tumor contributes to treatment resistance and tumor recurrence (2,3), even in the absence of genetic mutations.

It has recently been shown, however, that radiation itself can induce DCCs to reprogram and transition to CSCs. For example, ionizing radiation (IR) was shown to reprogram differentiated breast cancer cells (DBCSCs) into induced breast cancer stem cells (iBSCS) by showing that IR reactivates the same transcription factors in differentiated breast cancer cells that reprogram differentiated somatic cells into induced pluripotent Stem (iPS) cells (4). Moreover, the data suggests that the overexpression of Oct4 could be one possible mechanism behind radiation-induced reprogramming.

In addition, convincing evidence has suggested that feedback regulatory mechanisms inherited from normal tissues can also be playing a role in cancer, even if the feedback is not necessarily normal (5, 6). In heathy tissues, feedback has been recognized as a key component of growth control (7). In particular, tissue-specific signals affect the behaviors of stem, and non-stem cells. Classic examples are TGFb superfamily members, such as activin or GDF8, which are known to negatively regulate stem and non-stem division rates and stem self-renewal probability (7, 26). Such feedback regulation forms the basis of a powerful integral control strategy for maintaining homeostasis and rapid

regeneration of tissues after injury (8). In tumors, feedback regulation can significantly affect progression and response to treatment (8).

Mathematical modeling is ideally poised to investigate the response of tumors to IR, taking into account feedback regulation and reprogramming, in order to optimize therapeutic response. For example, in (7) the effect of the reprogramming was investigated, and it was suggested that reprogramming can fuel tumor growth, progression and treatment resistance. However, feedback regulation of cell behaviors was not considered. In a model of chemotherapy for human bladder cancer, negative feedback on CSC division rates, together with a wound-healing response that activates quiescent CSCs, results in CSC enrichment (9). In (10), a comprehensive analysis was performed to identify which types of regulatory feedback result in CSC enrichment. It was found that that negative feedback on the CSC division rate or positive feedback on the non-CSC (differentiated stem cell, DCC) death rate can lead to enrichment. The extent of CSC enrichment is determined by the CSC death rate and CSC self-renewal probability and by the feedback strength. In (14), a dual-compartment linear quadratic model of cell survival was introduced to account for the differential responses of CSCs and DCCs to IR and an ordinary differential equation model of tumor growth was used to investigate the response to radiotherapy using several fractionation schedules and several tumor types. Surprisingly, it was found that for glioblastoma (GBM), hypofactionation led to worse outcomes than traditional therapy fractionation schedules. In contrast, for other tumor types, such as non-small cell lung cancer (NSCLC), hypofractionation led to better outcomes. This work was later extended to include the effect of reprogramming (15) although neither (14) nor (15) considered the effect of feedback. In this thesis, we develop

a mathematical model to investigate the effect of feedback and reprogramming on radiation therapy outcomes. While the model is general, we focused on GBM.

GBM is the most common form of brain cancer that presents unique treatment challenges and has abysmal survival rates. GBM has an incidence of two to three per 100,000 adults per year and accounts for 52% of all primary brain tumors (11). The standard of care treatment involves surgically removing the tumor followed by radiotherapy and chemotherapy (27). In spite of such aggressive treatments, GBM almost always recurs, typically close to the original tumor site.

Unfortunately, the overall median survival for GBM patients is only 14 months (11,12). Because of this, numerous alterations in dose fractionation and escalation schemes have been attempted to improve treatment outcome and reduce treatment duration. Examples include accelerated hyper-fractionated treatment and hypo-fractionated treatment. Studies have shown, however, that such variable dosing regimens provide GBM patients no significant benefit in overall survival or durable local control (13).

In this work, we seek to understand how radiation therapy, radiation-induced reprogramming and feedback regulation interact to influence treatment responses of GBM tumors and to assess the effect of different treatment schedules. We follow the framework developed in (14,15). In particular, we use an ordinary differential equation (ODE) model that incorporates the distinct radiosensitivies of CSCs and DCCs using a dual-compartment linear quadratic (DLQ) model, reprogramming induced by IR, and negative feedback regulation of CSC division rates and self-renewal probabilities.

2. METHODS AND MATERIALS

This study involves three major components. First, a system of ordinary differential equations (ODE) is used to simulate tumor growth and the dynamic interaction between CSC and DCC populations. Second, we model the effect of radiotherapy on CSCs and DCCs using a dual-compartment LQ (DLQ) model (14). Third, we model reprogramming by assuming a dose-dependent population shift from DCCs to CSCs (15).

2.1 ODE model

The interplay between CSCs and DCCs is modeled using an ODE system that accounts for cell division in both compartments, transition from CSCs to DCCs and cell death. The model is:

$$\dot{U}(t) = (2P - 1)m_u U(t) - a_u U(t)$$

$$\dot{V}(t) = 2(1 - P)m_u U(t) + m_v V(t) - a_v V(t)$$

Equation 2-1

where U(t), V(t) are the numbers of CSCs and DCCs. CSCs divide at a rate m_u. At the population level, this results in either two daughter CSCs with probability P or two DCCs with probability $1 - P$. The growth rate of DCCs is m_v and the apoptosis(death) rates of CSCs and DCCs are a_u, a_v, respectively. Following (8), we assume that DCCs produce factors that negatively feedback CSC division rates and self-renewal probability:

$$m_u = \frac{\bar{m}_u}{1 + hV^k}, \quad m_v = \frac{\bar{m}_v}{1 + qV^r}, \quad P = \frac{\bar{P}}{1 + lV^n}$$

Equation 2-2

where $\bar{m}_u$, $\bar{m}_v$ and $\bar{P}$ are the intrinsic division rates of CSCs and DCCs and the self-renewal probability of CSC in the absence of any feedback. The feedback gains

h, q, l and exponent k, r, n control the strength of the inhibitory signals. We incorporate this negative feedback regulation into our ODE model.

2.2 Radiotherapy Model

A simple way to model the effect of radiosensitivity is the single-compartment linear quadratic (SLQ) model, which gives the survival fraction (SF) as a function of dose. The form is given below in Equation 2-3 for a single fraction of treatment:

$$SF(d) = e^{-\alpha d - \beta d^2}$$

Equation 2-3

where α and β are the linear and quadratic radiosensitivity parameters, and d is the fractional dose. However, the ability of the SLQ model to explain the response to stereotactic ablative body radiotherapy (SABR) dose has been challenged. Additionally, (14) suggests that the DLQ model is more suited to model the effect of IR in heterogenous tumors. Distinct radiosentsitivities of the CSC and DCC compartments specific to GBM are included in the DLQ model, which is given below:

$$SF(d) = Fe^{-\alpha_{CSC} d - \beta_{CSC} d^2} + (1 - F)e^{-\alpha_{DCC} d - \beta_{DCC} d^2}$$

Equation 2-4

where F is the fraction of CSCs in the total tumor number and $\alpha_{CSC}, \beta_{CSC}, \alpha_{DCC}$ and β_{CSC} describe the linear and quadratic radiobiological properties of each compartment. Least-squares fitting of the model was performed on diverse human cancer cell lines in (15), including U373MG (GBM), and the resulting parameters are adopted in this study. To compare doses, we use the biological effective doses (BED) which is given in Equation 2-5.

$$BED = nd \times \left(1 + \frac{d}{\alpha/\beta}\right)$$

Equation 2-5

with n, d and α/β representing the number of fractions, dose size, and the effective ratio of linear and quadratic sensitivities from SLQ model, respectively (14). In particular, we consider different n and d but match the BED.

Increasing evidence suggests that a portion of the DCC population reprograms back into CSCs after radiation exposure and the reprogramming rate is proportional to the dose. Accordingly, a reprogramming term is introduced into the model via a transfer of cells from the DCC compartment into the CSC compartment, following (15). In particular, after one application of radiotherapy, the surviving populations are modeled as:

$$U_S(t) = Ue^{-\alpha_{CSC}d_i - \beta_{CSC}{d_i}^2} + cd_iV$$

$$V_S(t) = Ve^{-\alpha_{DCC}d_i - \beta_{DCC}{d_i}^2} - cd_iV$$

Equation 2-6

where U_S and V_S are the surviving cell number after radiotherapy, U and V are the compartmental cell numbers prior to the application of IR. d_i is radiation dose applied to both CSCs and DCCs at the ith fraction, and c is the reprogramming coefficient. A full schematic of our ODE radiotherapy model is presented in Figure 2-1.

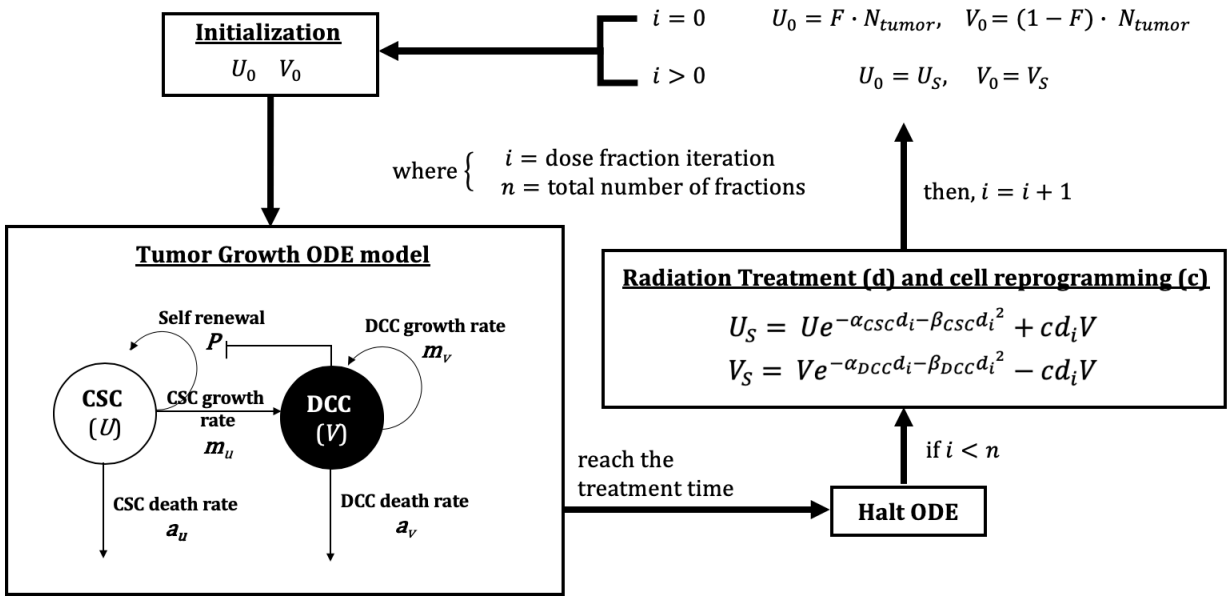

Figure 2.1: Schematic of algorithm ODE model (left) and DLQ and reprogramming model (right)

The reprogramming coefficient is determined based on a linear regression of the percentage of radiation-induced CSCs from DCCs in GBM, which is shown in Figure 2.2 (14).

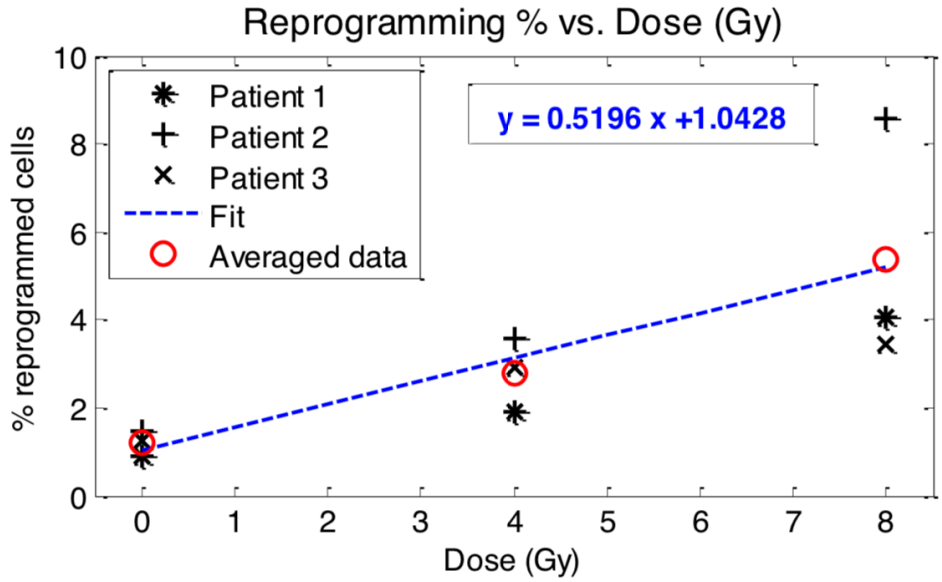

Figure 2.2: The percentage of reprogrammed cells with respect to dose received. Linear regression is used to determine the reprogramming coefficient – the slope of the dashed line. Adapted from (14)

In Figure 2-2, red circles represent the average data of three patients. The slope of the dashed line is the reprogramming coefficient c, that is utilized in our simulation. The parameters we used which correspond to GBM are shown in Table 2.1.

ODE parameters				Radiation therapy parameters					
N_{tumor}	m_u	m_v	a_v	F	α_{CSC}	β_{CSC}	α_{DCC}	β_{DCC}	c
4.2×10^9	0.1777	0.1777	0.0355	0.016	0.01	1.77E-07	0.125	0.028	5.196E-03

Table 2.1: ODE and Radiotherapy simulation parameters, which correspond to GBM

3. RESULTS

3.1 The Effect of the feedback

In this section, we study the effect of the feedback with and without reprogramming. Under the assumption that CSCs have unlimited replicative potential, the death rate of CSCs was set to 0. Following (16) , the intrinsic growth rates of CSC and DCC ($\bar{m}_u, \bar{m}_v$) are set to $ln(2)/T_{pot}$ 1/day, where T_{pot} is the tumor potential doubling time of malignant brain tumors. Basic self-renewal probability $\bar{P}$ is set to be 0.505 which is typically used in previous studies to maintain a dynamic equilibrium of CSCs and DCCs (14,16,17). The total tumor cell number is set to be 4.2×10^9 at time t = 0. The tumors are grown using the ODE model until time t = 100 after which conventional fractionated IR treatment (2Gy × 30) is applied and the system is simulated over a long time period afterwards. The results are shown in Figure 3.1.

In Figure 3.1, the green curves correspond to untreated tumors (solid denotes DCCs while dashed denotes CSCs). The black curves show the results assuming when there is no reprogramming while the red curves show the results when there is reprogramming.

Without feedback (Figure 3.1A), the DCC populations increase exponentially while the CSCs only increase slowly. Reprogramming induces a jump in the CSC population after treatment (see inset). Without reprogramming, the fraction of CSCs in the tumor tends to zero after spiking during the therapy (see black curves in supplementary Figure S1A).

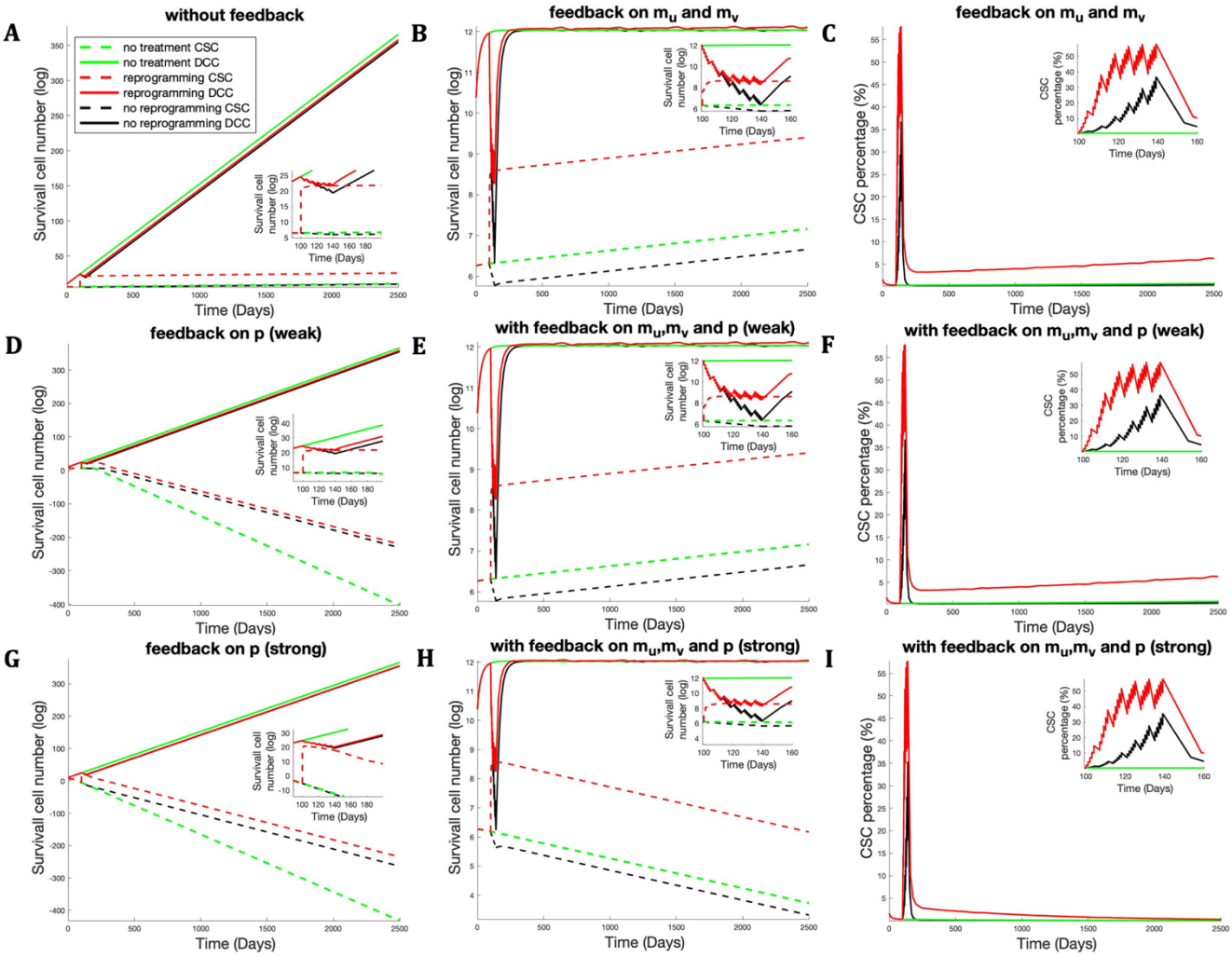

Figure 3.1: Treatment dynamics in the presence of negative feedback on cell division rates (m_u and m_v) and self-renewal probability P, as labeled.

When there is feedback on CSC and DCC division rates (Figure 3.1B), radiation treatment dramatically reduces the DCC populations and leads to a quasi-equilibrium (actually the DCCs increase slowly over time). The CSC populations grow rapidly during treatment when reprogramming is present, there is a significant increase in CSC population compared to the untreated case. Interestingly, if there is no reprogramming, the CSC population is less than that in the untreated tumor. The corresponding CSC percentages are shown in Figure 3.1C. It is clear that when there is feedback and reprogramming, the CSC fraction increases even a long time after the treatment was stopped.

When there is feedback on self-renewal probability only (Figure 3.1D and G), DCC populations exponentially increase, while the CSC numbers decrease to zero. With weak feedback (Figure 3.1D), the CSC numbers remain constant before treatment. After treatment, a jump in CSC population due to reprogramming is observed, whereas there is no jump in CSC population without reprogramming (see inset). Even with the jump, the CSC population exponentially decays. With strong feedback (Figure 3.1G), the CSC population decreases continually in time, although there is a boost in CSC numbers due to reprogramming after treatment. Because of exponential growth of DCC and exponential decay of CSCs, the CSC fractions tends to zero at long times (supplementary Figure S1B and SC, also could be seen in Figure 3.2 F black line). This demonstrates that feedback on self-renewal probability can lead to decrease of the CSC populations and fractions.

With weak feedback on self-renewal probability combined with feedback on division rates (Figure 3.1E-F), the dynamics of CSCs and DCCs behave analogously to system with feedback solely on division rates.

When strong feedback on self-renewal is combined with feedback on division rates (Figures 3.1H-I), the dynamics of the DCCs is almost identical to that with weak feedback (Figure 3.1E), while the evolution of CSCs is entirely different (Figure 3.1E). When the reprogramming is present, the CSC populations rapidly grow directly after treatment, but the number of CSCs decreases exponentially once the treatment is completed. If there is no reprogramming, the CSC number is less than untreated tumor. Therefore, the CSC fraction tends to zero, shown in Figure 3.1I.

Figure 3.2 shows the corresponding effective division rates of CSC and DCC (Figure 3.2A) and the effective self-renewal probabilities (Figures 3.2B-D) from Equation 2-2 for the simulations shown in Figure 3.1. When there is feedback on division rates (Figure 3.2A), the division rates decrease to a constant in the untreated tumor because of the negative feedback. This is because the DCC population changes slowly at long times. When the tumor is treated, there is spike increase in division rates because DCCs are being killed off, which relieves the CSCs from the negative feedback. However, as the DCC population rebounds, the division rates decrease and reach levels close to untreated tumor.

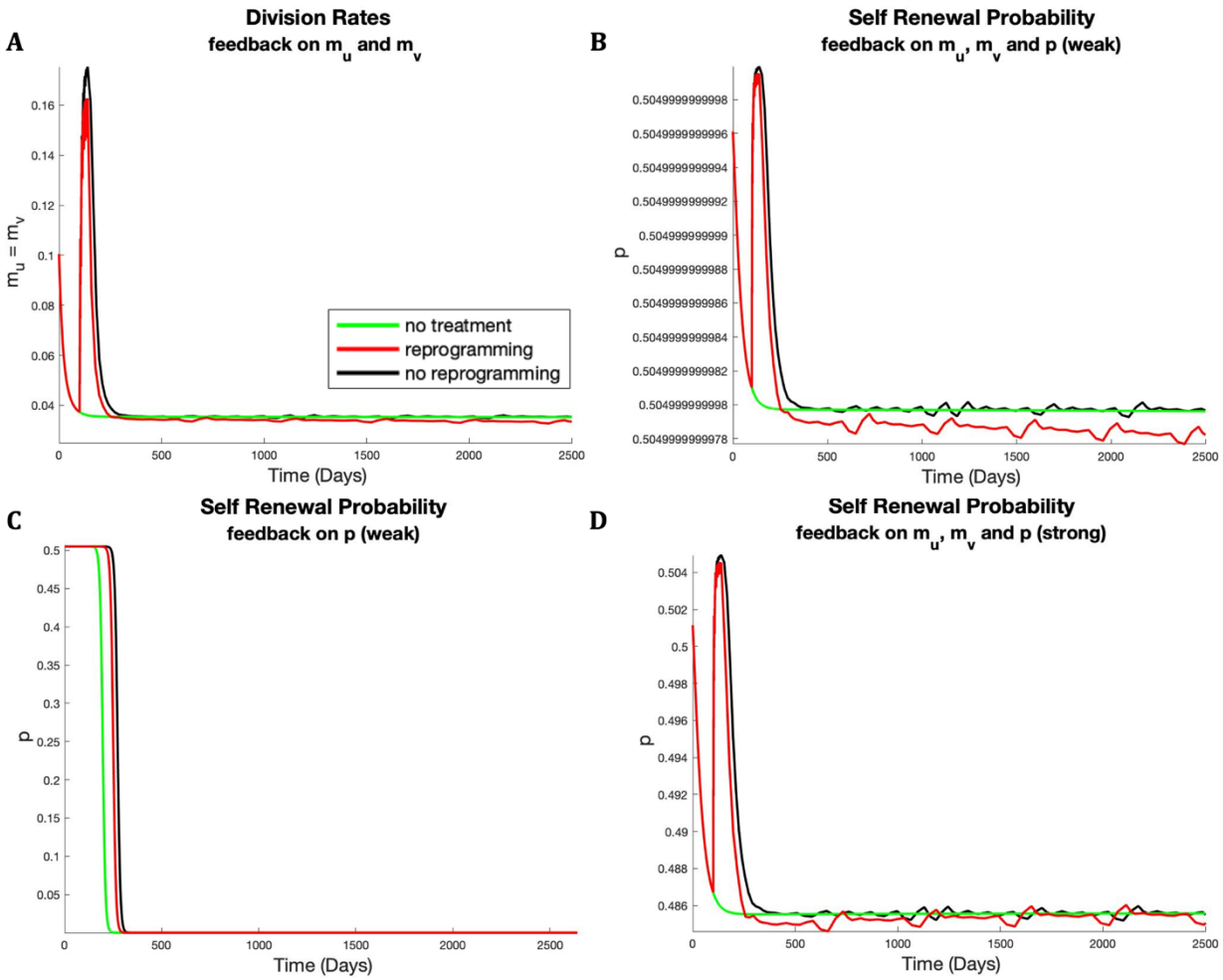

Figure 3.2: Effective division rate sand self-renewal probabilities in presence of negative feedback corresponding to the simulation shown in Figure 3.1

We see from Figure 3.2B that the reason that the CSC numbers increase in Figure 3.1E, where weak negative feedback on the self-renewal probability is combined with feedback on division rates, is that the effective self-renewal probability stays above 0.5, which induces accumulation of CSCs. In contrast, Figure 3.2C-D shows that the reason that CSC numbers are declining in Figure 3.1D, G and H, where the feedback on the self-renewal probability is strong, is that $p < 0.5$, so the CSC do not self-renew and instead differentiate (see also Supplementary Fig. S2A).

3.2 The Effect of dose fractionation

Using parameters for GBM, aside from conventionally fractionated schemes of 2Gy × 30 days, various alterations in dose fractionation and escalation schemes with the same BED were applied to test treatment outcomes. Accelerated hyper-fractionated twice a day of 1 to 1.5 Gy fractions (18-20), hypofractionated 3 to 6Gy (21-23) fractions schemes were implemented experimentally and no substantial benefit in overall survival or durable local control was observed (24). These treatments might have failed because of a lack of understanding of negative feedback and reprogramming. To maximize the treatment efficacy, we need to understand how negative feedback and reprogramming can influence treatment response using different doses and schedules. Assuming that there is negative feedback on division rates of CSCs and DCCs and weak feedback on self-renewal probability, we have simulated the dynamics of CSCs and DCCs. We have observed a difference in behavior with and without reprogramming.

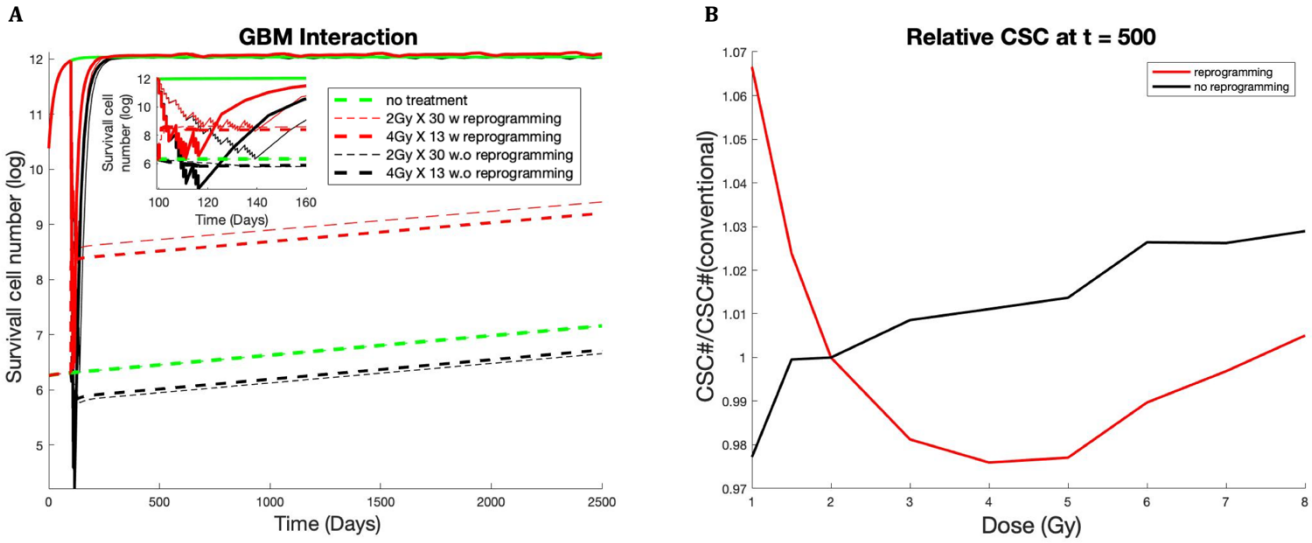

Figure 3.3: A: GBM populations with different fractionation schedules B: Relative numbers of CSCs at 500 with different fractionation schedules

In Figure 3.3A, different doses with the same BED are applied to GBM at t = 100 and the dynamics of CSCs and DCCs are simulated for a long time period. The green curves represent the untreated case, where solid lines are the DCC numbers and dashed lines are the CSC numbers. The black curves correspond to the cases in which there is no reprogramming and the red curves show the results when there is reprogramming (thin curves denote conventional treatment with 2Gy × 30 days while thick curves denote hypofractionation with 4Gy × 13 days). When there is reprogramming, the CSC populations grow rapidly and the increase in the CSC numbers relative to the untreated simulation is more pronounced. The CSC numbers with conventional treatment are relatively higher than that with hypo-fractionated treatment. This is in contrast to the case without reprogramming where the CSC population is smaller than that in the untreated tumor. In addition, the CSC populations treated with hypofractionation is slightly higher than that treated conventionally, which suggests conventional therapy would be a better choice for tumor control, although all the treated cases end up following a trajectory similar to untreated tumor.

We next investigate the relationship between the CSC population and the dose size with and without reprogramming. In particular, we consider the number of CSC at t = 500 relative to that using conventional treatment (2Gy × 30days). The results are shown in Figure 3.3B. Without reprogramming (black), the CSC population is roughly a linear function of IR dose. In contrast, when there is reprogramming (red), the CSC number is a nonlinear function of the dose sizes and has a minimum near the 4Gy × 13 days treatment schedule. This suggests that there is an optimal choice of fractionation schedule, e.g., hypofractionation (approximately 4Gy × 13 days), that results in the lowest relative CSC number.

3.3 The Effect of repeated treatment

We use same mathematical model to investigate the effect of repeated treatment. Assuming that there is negative feedback and reprogramming, we applied therapy repeatedly for different dose schedules and investigated the resulting dynamics of the system.

As before, the tumor is grown to time t=100 and IR treatment is started. Further, IR is applied every 400 days (Figure 3.4) for four cycles. System with negative feedback on division rates combined with weak negative feedback on self-renewal probability with reprogramming is simulated for long time period afterward. In Figure 3.4 A, every

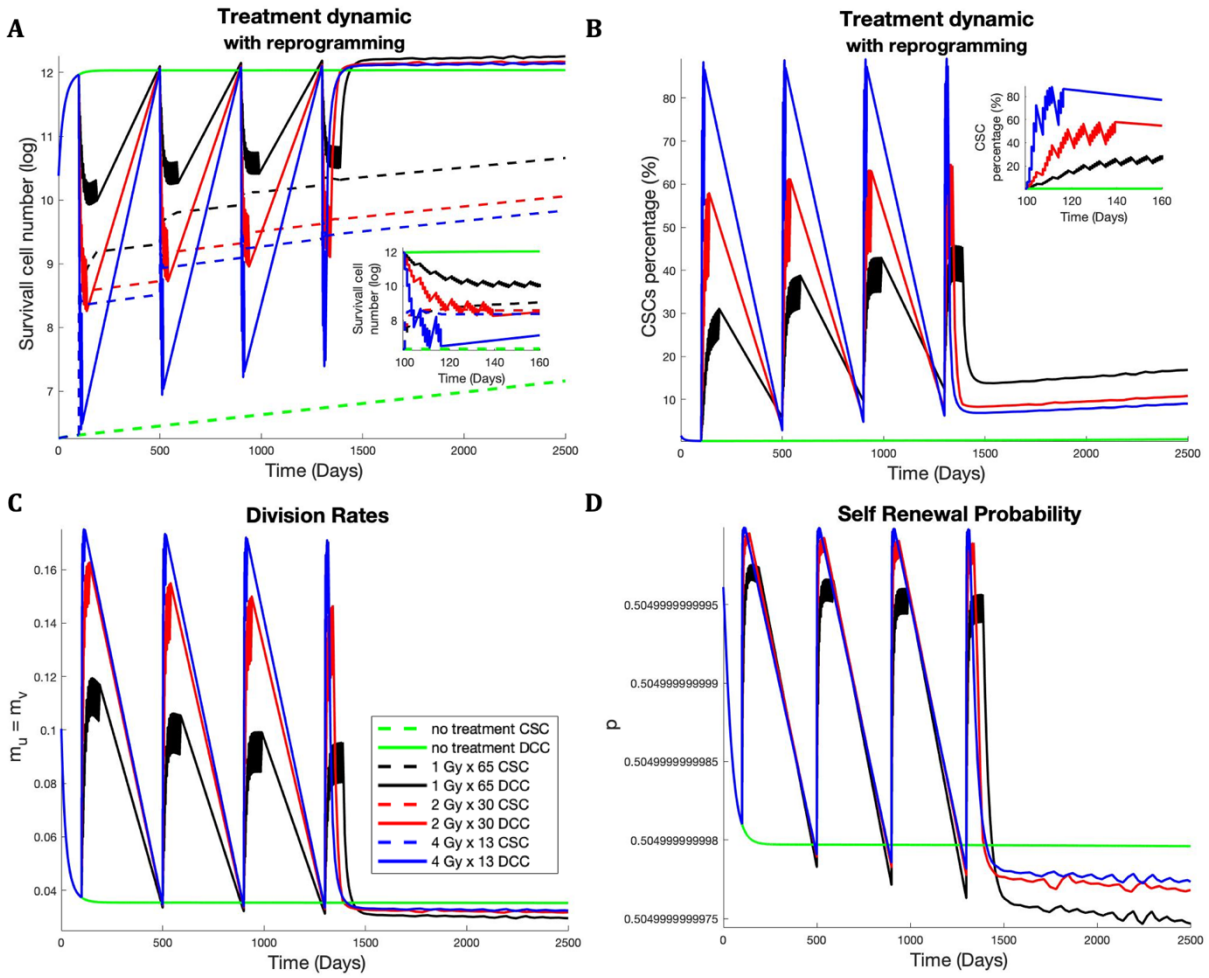

Figure 3.4: Repeated treatment of dynamics in the presence of negative feedback (weak negative feedback on self-renewal probability) and reprogramming

time the treatment is applied, the CSC numbers rapidly increase and then continue to increase gradually until the next treatment is applied. Each application of IR treatment temporarily reduces tumor sizes, but after each therapy cycle ends, the tumor sizes increase rapidly, driven by resistant CSCs, to levels even above those for untreated tumors. The case using the hyper-fractionated scheme with 1 Gy × 65 results the most dramatic increases of the CSC numbers. The best response is obtained using the 4Gy × 13 days schedule although the CSC percentages are still higher than the untreated case.

Figures 3.4 C-D show the effective division rates of CSCs and DCCs and the self-renewal probabilities can be found in Figure 3.4A. In Figure 3.4C, because of the negative feedback on division rates, at every cycle of treatment, there is a spike increase in division. The death of the DCCs relieves the feedback on the CSCs but as soon as the DCC populations rebound, the division rates decrease and reach a lower level than the untreated case. Even with the negative feedback on self-renewal probability, because feedback is weak, the self-renewal probability stays slightly above 0.5 which induces slow growth of the CSC populations.

Assuming that there is negative feedback and the reprogramming, repeating the radiotherapy can induce the enrichment of CSCs which can lead to resistance and a loss of sensitivity to radiotherapy.

4. Discussion and Conclusion

Experimental observations indicate that the percentages of CSCs are positively correlated with overall tumor growth and resistance to treatment (4). Focusing on radiation treatment of GBM tumors, we investigated the effect of feedback on CSC division and self-renewal probabilities, reprogramming, and treatment with different dose scheduling on the CSC populations and overall tumor size. Using, an ODE model, which is coupled with a model for radiation survival (DLQ) and reprogramming, we find sustained CSC enrichment from radiotherapy leads to emergence of resistance and a loss of sensitivity to treatment.

From the mathematical model with specific radiosensitivities to GBM, we suggest that the presence of negative feedback loops and reprogramming in tumors as significant factors of tumor sensitivity to radiotherapy in the context of stem cell-based resistance. When reprogramming was considered, we demonstrated that feedback on cell division rates induces long-term enrichment of CSCs while the effect of feedback on self-renewal probabilities results only in short-term CSC enrichment. Therefore, repeating treatments to solid tumors induces a pronounced expansion in the number of CSCs and this induce a loss of sensitivity to radiotherapy. Using the model, we investigated the relationship between CSC numbers and IR dose in GBM. When there is no reprogramming, the numbers of CSC increase roughly linearly with the dose while there is optimal choice of dose fractionation if there is reprogramming.

In conclusion, we discover that long-term increases in the CSC fractions in tumor are associated with feedback on cell division rates by factors made by the DCC numbers when reprogramming is present. If the treatment is cycled, the CSC numbers continually increase because of reprogramming. This phenomenon leads to emergence of resistance that is non-

genetic in its origin. Accordingly, inhibiting reprogramming and increasing strength of negative feedback can improve the effectiveness of radiotherapy.

In future work, we can test this study in different cancer cell types such as NSCLC as (14). Also, we can formulate the optimization problem on dose fractionation with different BED. Furthermore, studying spatial limitation on this study might be needed to study how much feedback can diffuse spatially. Lastly, we can test this theoretical result in an experiment. We can prescribe retinoic acid (RA) to inhibit the proliferation of tumors and to reduce the self-renewal probability of CSCs (25).

REFERENCE

1. Pajonk F, Vlashi E, McBride WH. Radiation resistance of cancer stem cells: the 4 R's ofradiobiology revisited. Stem Cells. 2010;28(4):639-648.
2. Ogawa K, Yoshioka Y, Isohashi F, Seo Y, Yoshida K, Yamazaki H. Radiotherapy targeting cancer stem cells: current views and future perspectives. Anticancer research.2013;33(3):747-754
3. Woodward WA, Chen MS, Behbod F, Alfaro MP, Buchholz TA, Rosen JM. WNT/beta-catenin mediates radiation resistance of mouse mammary progenitor cells. Proc Natl Acad Sci U S A. 2007;104(2):618-623.
4. Lagadec C, Vlashi E, Della Donna L, Dekmezian C, Pajonk F. Radiation-induced reprogramming of breast cancer cells. Stem Cells. 2012;30(5):833-844.
5. Kurtova, A.V., Xiao, J., Mo, Q., Pazhanisamy, S., Krasnow, R., Lerner, S.P., Chen, F., Roh, T.T., Lay, E., Ho, P.L., Chan, K.S., 2015. Blocking PGE2-induced tumour repopulation abrogates bladder cancer chemoresistance. Nature 517, 209–213. doi:10.1038/nature14034.
6. Rodriguez-Brenes, I.A., Kurtova, A.V., Lin, C., Lee, Y.C., Xiao, J., Mims, M., Chan, K.S., Wodarz, D., 2017. Cellular hierarchy as a determinant of tumor sensitivity to chemotherapy. Cancer Res. 77, 2231–2241. doi:10.1158/0008-5472.CAN-16-2434.
7. Leder, K., Holland, E.C., Michor, F., 2010. The therapeutic implications of plasticity of the cancer stem cell phenotype. PLoS One 5, e14366. doi:10.1371/journal.pone. 0014366

8. Youssefpour H, Li X, Lander AD, Lowengrub JS. Multispecies model of cell lineages and feedback control in solid tumors. 2012;304:39-59
9. Ignacio A, Rodriguez-Brenes, et al. Cellular Hierarchy as a determinant of tumor sensitivity to Chemotherapy
10. Lora D. Weiss, P.van den Driessche, John S. Lowengrub, Dominik Wodarz, and Natalia L. Komarova. Effect of feedback regulation on stem cell fractions in tissues and tumors: understanding chemoresistance in bladder cancer. BioRxiv 2019;
11. Eric C. Holland. Gliobalstoma multiforme: The terminator 2000 Jun 6; 97(12): 6242–6244.
12. Adamson C, Kanu OO, Mehta AI, et al. Glioblastoma multiforme: a review of where we have been and where we are going. Expert Opin Investig Drugs. 2009;18(8):1061-1083.
13. Chan JL, Lee SW, Fraass BA, et al. Survival and failure patterns of high-grade gliomas after three-dimensional conformal radiotherapy. J Clin Oncol. 2002;20(6):1635-1642.
14. Victoria Y. Yu, Dan Nguyen, et al. Incorporating cancer stem cells in Radiation therapy treatment response modeling and the implication in Glioblastoma Multiforme treatment resistance. International Journal of Radiation oncology
15. Garcia LM, Wilkins DE, Raaphorst GP. Alpha/beta ratio: A dose range dependence study. Int J Radiat Oncol Biol Phys. 2007;67(2):587-593.
16. Bachman JW, Hillen T. Mathematical optimization of the combination of radiationand differentiation therapies for cancer. Front Oncol. 2013;3:52.

17. Hillen T, Enderling H, Hahnfeldt P. The tumor growth paradox and immune system-mediated selection for cancer stem cells. Bull Math biol 2013;75:161-184
18. Shrieve DC, Wara WM, Edwards MS, et al. Hyperfractionated radiation therapy for gliomas of the brainstem in children and in adults. Int J Radiat Oncol Biol Phys. 1992;24(4):599-610.
19. Nieder C, Nestle U, Ketter R, et al. Hyperfractionated and accelerated-hyperfractionated radiotherapy for glioblastoma multiforme. Radiat Oncol Investig. 1999;7(1):36-41.
20. Deutsch M, Green SB, Strike TA, et al. Results of a randomized trial comparing BCNUplus radiotherapy, streptozotocin plus radiotherapy, BCNU plus hyperfractionated
21. Floyd NS, Woo SY, Teh BS, et al. Hypofractionated intensity-modulated radiotherapy for primary glioblastoma multiforme. Int J Radiat Oncol Biol Phys. 2004;58(3):721-726.
22. Bauman GS, Gaspar LE, Fisher BJ, Halperin EC, Macdonald DR, Cairncross JG. A prospective study of short-course radiotherapy in poor prognosis glioblastoma multiforme. Int J Radiat Oncol Biol Phys. 1994;29(4):835-839.
23. Ford JM, Stenning SP, Boote DJ, et al. A short fractionation radiotherapy treatment for poor prognosis patients with high grade glioma. Clin Oncol (R Coll Radiol). 1997;9(1):20-24.
24. Laperriere N, Zuraw L, Cairncross G, Group CCOPGIN-ODS. Radiotherapy for newly diagnosed malignant glioma in adults: a systematic review. Radiother Oncol. 2002;64(3):259-273.

25. Crowe DL, Kim R, Chandraratna RA. Retinoic acid differentially regulates cancer cell proliferation via dose dependent modulation of the mitogen-activated protein kinase pathway. Mel Cancer Res. 2003;1(7) 532-40
26. Kimberly K. Gokoffski et al. Activin and GDF collaborate in feedback control of neuroepithelial stem cell proliferation and fate. Development. 20199:138(19) 4131 - 4142
27. Adamson C, Kanu OO, Mehta AI, et al. Glioblastoma multiforme: a review of where we have been and where we are going. *Expert Opin Investig Drugs*. 2009;18(8):1061-1083.

SUPPLEMENTARY

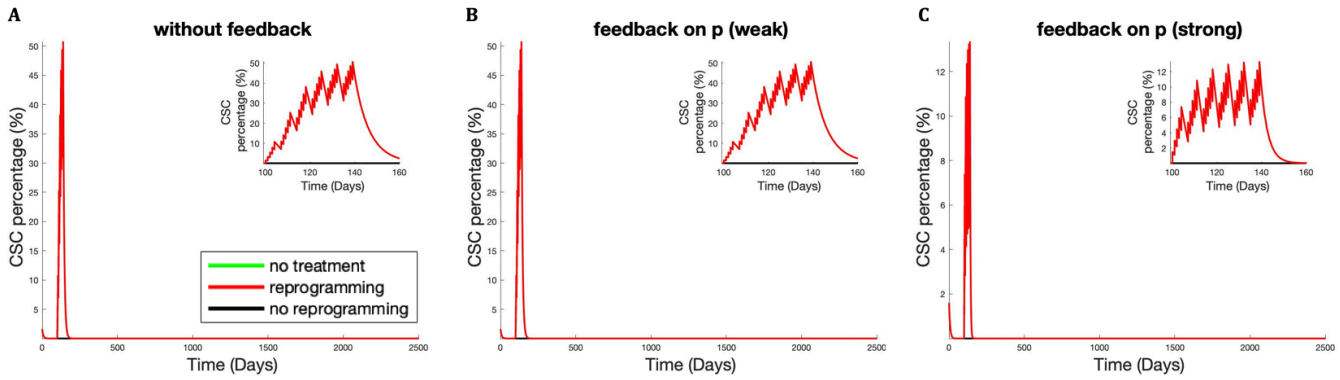

Figure S1. CSC percentage in absence and presence of negative feedback on self-renewal probability *P*.

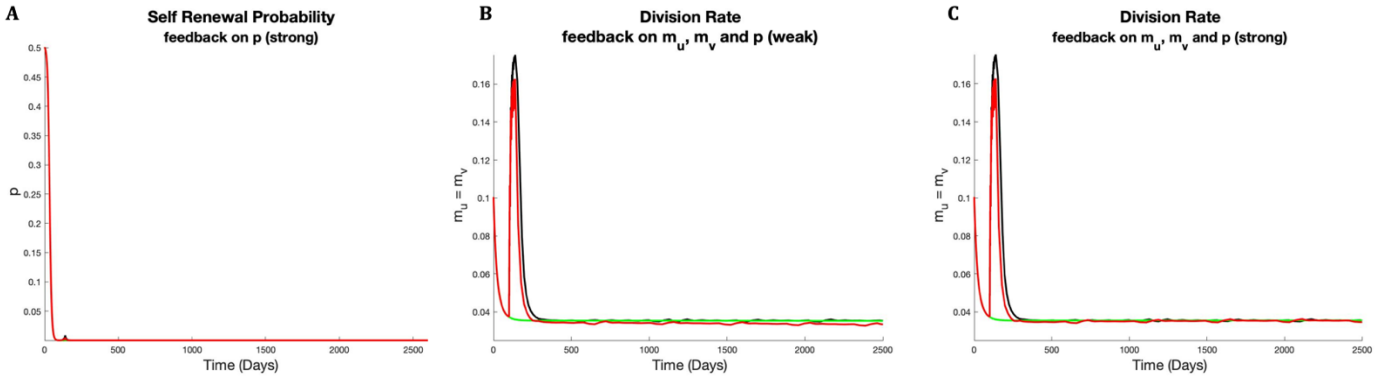

Figure S2. Effective division rates and self-renewal probability in presence of negative feedback corresponding to simulation shown in Figure 3.1.

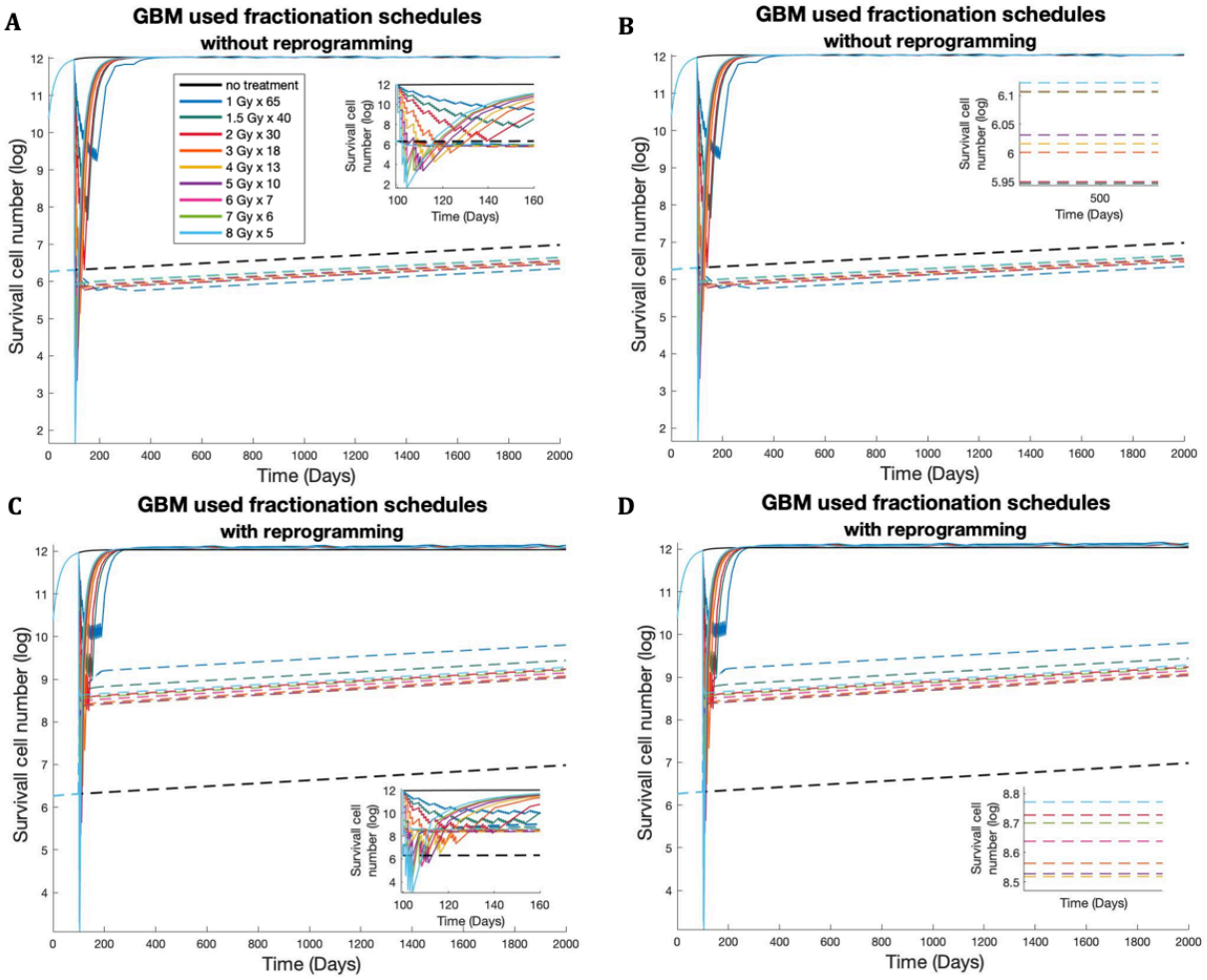

Figure S3. GBM populations with different fractionation schedules. Hyper-fractionated treatment (1, 1.5Gy), conventional treatment (2Gy) and hypo-fractionated treatment (3, 4, 5, 6, 7, 8Gy) has been applied GBM.

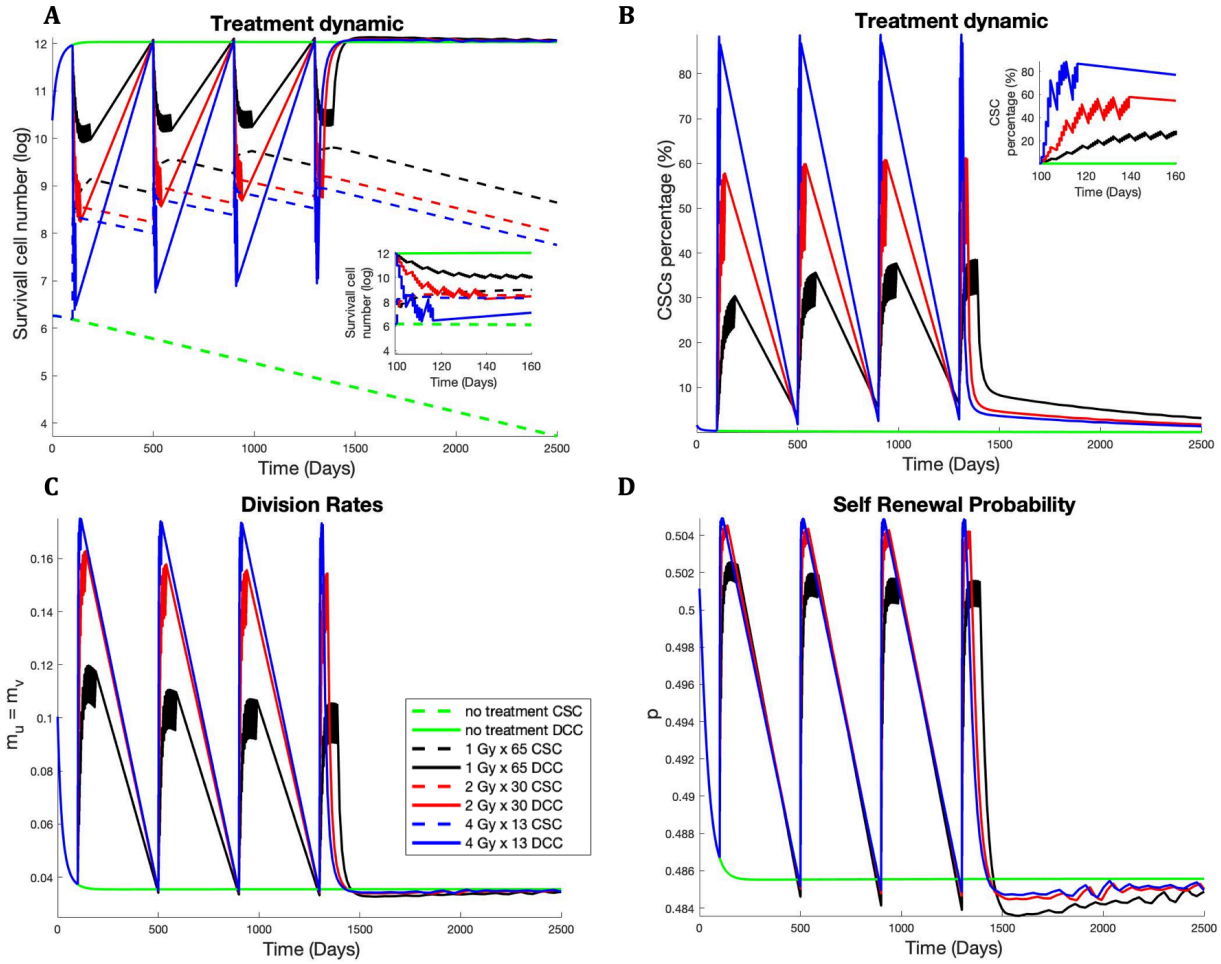

Figure S4. Repeated treatment of dynamics in the presence of negative feedback (strong negative feedback on self-renewal probability) and reprogramming